# Indirect Torque Control of Synchronous Machines via Feedback Linearization

Zoltán Téczely
*Department of Control Engineering and Information Technology*
*Budapest University of Technology and Economics*
Budapest, Hungary
teczely@iit.bme.hu

Dávid Somogyi
*Faculty of Information Technology and Bionics*
*Pázmány Péter Catholic University*
Budapest, Hungary
somogyi.david@itk.ppke.hu

***Abstract*—Actuator characteristics, particularly actuator dynamics, play a pivotal role in mechatronic control systems. The inherent nonlinearity in synchronous machines may reduce the closed-loop performance of any high-level control system, especially in industrial applications, where system sizing is performed with a heavy emphasis on cost-optimisation, forcing the actuator to consistently reside in marginal operating states. The performance of the motor can be described by its reactiveness over the feasible operating points, yielding a nonlinear character. Typically, motor performance decreases with increasing rotor speed, and in turn, the interconnected high-level control system may be impacted by abruptly occurring oscillations or may become unstable. To counter this effect, feedback linearization is proposed for a Permanent Magnet Synchronous Motor (PMSM) with torque control objective. To maintain exact linearizability of the motor and, critically, to account for sudden load variations, torque tracking is ensured indirectly by a derived rotor speed reference. Such a control scheme is intended to turn a nonlinear motor character into a seemingly linear one to which linear high-level control techniques are more easily applicable. This motor control loop is then embedded into an example electromechanical power steering system (EPS). To validate the proposed approach, its superiority is shown over the standard linear motor control in terms of linear character and consistency within the prescribed operating range, significantly improving overall behaviour in a high-level control system.**

***Index Terms*—Feedback linearization, Actuator dynamics, Nonlinear control**

## I. Introduction

Permanent Magnet Synchronous Motors are often utilized in mechatronic systems for their high customizability, cost-effectiveness, and high performance. The traditional way these motors are controlled is the so-called Field-Oriented Control (FOC) [1], wherein the current phases of the stator are transformed into two orthogonal components. Most often, these components are controlled via linear PI controllers. Another technique recently gaining popularity is Direct Torque Control (DTC) [2], in which no such coordinate transformations take place, and no additional controller is needed.

Even though in FOC the phase currents are transformed into constant values through the Clarke-Park transformations, the control of these values remains a linear process in general. This results in nonlinear motor behaviour when observing dynamic response over various operating conditions. In itself, this might not pose a big problem for the motor, but for any high-level mechatronic application, this alternating behaviour can result in oscillations, performance loss, or even instability. This nonlinear character is further enhanced by the commonly employed field-weakening method [3], in which higher rotor speeds can be achieved by reducing the available motor torque, ultimately resulting in a nonlinear actuator power curve.

Partly to reduce the effect of nonlinear motor dynamics, in recent times, nonlinear control techniques have been applied to PMSMs combined with FOC [4] and DTC [5].

PMSMs are generally suitable for a range of feedback linearization techniques, of which possibly the most notable example is [6], who pair Active Disturbance Rejection Control (ADRC) with feedback linearization.

On the other hand, actuator control methods are usually studied as standalone entities rather than building blocks of a more complex control system. The interconnection between the motor and the high-level system can be described by the well-known small gain theorem [7], giving rise to a series of controller performance-related trade-offs. Driven by the same reason, the actuator nonlinearity described in this paper has been investigated in [8] for the same PMSM motor from a different perspective. In that work, the authors presented Linear Parameter-Varying (LPV) controls on the high-level application as a countermeasure for the inherent nonlinearity in the motor. Opposed to that, the current work is an effort to remove the nonlinear character where it appears in the system.

The primary contribution of this paper is a method to apply feedback linearization to a PMSM with torque control objective. The proposed approach takes into account the uncertain character of the load and applies to arbitrary load variations limited only by the estimation bandwidth. This structure is then embedded into an example steering system, wherein improved actuator characteristics, i.e. linear behaviour, significantly increase the feasible operating region.

The remainder of the paper is organised as follows: Section II. presents the mathematical model of the motor, while Sections III. and IV. include exact linearization applied to the motor and subsequent control, respectively. Section V. is concerned with the validation results, and Section VI. concludes the paper.

## II. Mathematical model of PMSM

This section introduces the system equations of the PMSM motor together with the characterisation of a real-life motor.

The mathematical model of PMSM under d-q coordinate system [9] reads

$$\begin{aligned} \dot{i_d} &= \frac{-Ri_d}{L} + i_q\omega + \frac{1}{L}u_d, \\ \dot{i_q} &= \frac{-Ri_q - \psi\omega}{L} - i_d\omega + \frac{1}{L}u_q, \\ \dot{\omega} &= \frac{3}{2}\frac{n_p\psi i_q}{J} - \frac{\beta\omega + T_l}{J}, \end{aligned} \tag{1}$$

where the state and input variables are $x = \begin{bmatrix} i_d & i_q & \omega \end{bmatrix}^T$ and $u = \begin{bmatrix} u_d & u_q & T_l \end{bmatrix}^T$, respectively. The first two equations describe the electrical dynamics of a PMSM, specifying how voltage and current in the stator windings generate a magnetic field that interacts with the rotor's permanent magnets to produce torque. The third equation captures the mechanical dynamics, describing how the generated torque translates into rotational motion, including inertia and damping terms.

Throughout the paper, the load input ($T_l$) is assumed to be nonzero, with slow variations compared to the system dynamics ($\dot{T}_l = 0$). For this reason, it is considered a non-controllable disturbance, therefore, it has to be estimated, which leads to its removal from the input matrix. The parameter values used in the simulation are given in Table I.

TABLE I: Variables and parameters of the motor model.

| Parameter | Interpretation | Value | Unit |
|---|---|---|---|
| $i_d, i_q$ | Currents in the d-q circuit | State | A |
| $\omega$ | Rotor speed | State | $\frac{\text{rad}}{\text{s}}$ |
| $L$ | Inductance ($L_d = L_q = L$) | $5 \cdot 10^{-5}$ | H |
| $R$ | Resistance | 0.006 | $\Omega$ |
| $n_p$ | Number of pair of poles | 5 | – |
| $\psi$ | Flux | 0.008 | $\frac{\text{Nm}}{\text{A}}$ |
| $J$ | Moment of inertia | $2.5 \cdot 10^{-4}$ | $\text{kg} \cdot \text{m}^2$ |
| $\beta$ | Viscous friction coefficient | 0.03 | $\frac{\text{Nm} \cdot \text{s}}{\text{rad}}$ |
| $u_d, u_q$ | Voltages of the d-q circuit | Input | V |
| $T_l$ | Load torque | Disturbance | Nm |

## III. Exact feedback linearization of PMSM

The following section describes the proposed exact linearization method applied to a PMSM motor. For a basic theoretical background, the reader is referred to [10].

As a motivation, the degradation in motor dynamics can be reduced if feedback linearization is applied to the PMSM model. After removal of the load from the input vector (resulting in $u = \begin{bmatrix} u_d & u_q \end{bmatrix}^T$), the necessary and sufficient conditions for feedback linearizability based on [10] are met if the measurement vector of the nonlinear system is $h(x) = \begin{bmatrix} i_d & \omega \end{bmatrix}^T$.

The model (1) admits the general input-affine form

$$\begin{aligned} \dot{x} &= f(x) + \sum_{i=1}^{n} g_i(x)u, \\ y &= h(x), \end{aligned} \tag{2}$$

with $u \in \mathbb{R}^n$ being the input vector and the functions are

$$\begin{aligned} f(x) &= \begin{bmatrix} \frac{-Ri_d}{L} + i_q\omega \\ \frac{-Ri_q - \psi\omega}{L} - i_d\omega \\ \frac{3}{2}\frac{n_p\psi i_q}{J} - \frac{\beta\omega + T_l}{J} \end{bmatrix}, \\ g(x) &= \begin{bmatrix} g_1(x) & g_2(x) \end{bmatrix} = \begin{bmatrix} \frac{1}{L} & 0 \\ 0 & \frac{1}{L} \\ 0 & 0 \end{bmatrix}, \\ h(x) &= \begin{bmatrix} h_1(x) & h_2(x) \end{bmatrix}^T = \begin{bmatrix} i_d & \omega \end{bmatrix}^T. \end{aligned} \tag{3}$$

We seek an adequate coordinate transformation that puts the system into normal form, and a feedback law that yields a linear input-output map from the linearized inputs $v$ to $y$.

### A. Coordinate transformation

Differentiating the outputs until the inputs appear explicitly leads to the *diffeomorphism* [10] $z = \Phi(x)$, in more detail

$$\begin{aligned} z_1 &= h_1(x) = i_d, \\ z_2 &= h_2(x) = \omega, \\ z_3 &= \mathcal{L}_f h_2(x) = \frac{3}{2}\frac{n_p\psi i_q}{J} - \frac{\beta\omega + T_l}{J}, \end{aligned} \tag{4}$$

where the notation $\mathcal{L}$ represents the Lie-derivative. In the new coordinates, introducing $v = \begin{bmatrix} v_d & v_q \end{bmatrix}^T$ as the vector of the new input variables, the system appears as

$$\begin{aligned} \dot{z}_1 &= v_d, \\ \begin{bmatrix} \dot{z}_2 \\ \dot{z}_3 \end{bmatrix} &= \begin{bmatrix} 0 & 1 \\ 0 & 0 \end{bmatrix} \begin{bmatrix} z_2 \\ z_3 \end{bmatrix} + \begin{bmatrix} 0 \\ 1 \end{bmatrix} v_q, \end{aligned} \tag{5}$$

i.e. the map from $v$ to $y$ is represented by a chain of integrators and is linear and controllable.

### B. Relative degree

We seek the linearizing feedback $u = A^{-1}(x)\left(-b(x) + v\right)$ such that the new input vector $v$ satisfies (5) where

$$b(x) = \begin{bmatrix} \mathcal{L}_f h_1 \\ \mathcal{L}_f^2 h_2 \end{bmatrix} = \begin{bmatrix} \frac{-Ri_d}{L} + i_q\omega \\ \left\{ \frac{3}{2}\frac{n_p\psi}{J}\left(\frac{-Ri_q - \psi\omega}{L} - i_d\omega\right) \right\} \\ \left\{ -\beta\left(\frac{3}{2}\frac{n_p\psi i_q}{J^2} - \frac{\beta\omega + T_l}{J^2}\right) \right\} \end{bmatrix} \tag{6}$$

and

$$A(x) = \begin{bmatrix} \mathcal{L}_{g_1} h_1 & \mathcal{L}_{g_2} h_1 \\ \mathcal{L}_{g_1}\mathcal{L}_f h_2 & \mathcal{L}_{g_2}\mathcal{L}_f h_2 \end{bmatrix} = \begin{bmatrix} \frac{1}{L} & 0 \\ 0 & \frac{3}{2}\frac{n_p\psi}{LJ} \end{bmatrix}. \tag{7}$$

The matrix $A$ is invertible, therefore, the system has a well-defined vector relative degree. Then, the feedback linearizing input is given by

$$\begin{aligned} u = \begin{bmatrix} u_d \\ u_q \end{bmatrix} &= A^{-1}(x)\left(-b(x) + v\right) = \\ &= \begin{bmatrix} Ri_d - Li_q\omega + Lv_d \\ \left\{ Ri_q + \psi\omega + Li_d\omega + \frac{L\beta i_q}{J} \right\} \\ \left\{ -\frac{2L\beta}{3\psi n_p J}(\beta\omega + T_l) + \frac{2}{3}\frac{LJ}{n_p\psi}v_q \right\} \end{bmatrix}. \end{aligned} \tag{8}$$

**Proposition 1.** *For the nonzero load case, the only option for exact feedback linearization of the model* (1) *in the input-affine form* (2) *is to select* $h(x) = \begin{bmatrix} i_d & \omega \end{bmatrix}^T$.

*Proof.* Let us investigate the following necessary conditions for exact feedback linearizability:

- $r = n$, that is, the vector relative degree must be equal to the dimension of the model
- The matrix $A$ in (7) must be nonsingular

If the first two states are measured $h(x) = \begin{bmatrix} i_d & i_q \end{bmatrix}^T$, the vector relative degree of the model is $r = 2$, since the inputs $u_d$ and $u_q$ appear explicitly in the corresponding state equation in (1), therefore the first requirement is violated.

If the second and third states are measured $h(x) = \begin{bmatrix} i_q & \omega \end{bmatrix}^T$, the relative degree increases to $r = 3$, since $\dot{i}_q$ explicitly depends on $u_q$ but we have to differentiate $\omega$ twice until $u_q$ appears. However, this way we reach the same input ($u_q$), which means, the matrix $A$ takes the form

$$A = \begin{bmatrix} 0 & * \\ 0 & * \end{bmatrix} \rightarrow \det A = 0,$$

that is, $A$ is singular, with $*$ representing nonzero elements.

The motor model has a vector relative degree equal to the model dimension ($r = n = 3$) with a nonsingular $A$ matrix only if $h(x) = \begin{bmatrix} i_d & \omega \end{bmatrix}^T$.

□

**Remark 1.** *In a typical motor, all three states are measured, however, they are not necessarily included in the feedback linearization scheme as measured quantities. For full-state feedback control, we need $y = x$, hence, in practice, all state measurements are available.*

**Remark 2.** *For practical purposes, the squareness assumption, that is, $dim(g) = dim(h)$, can be relaxed. The nonsquare nature of matrix $A$ could be countered by taking the Moore-Penrose pseudoinverse.*

## IV. PMSM Control via feedback linearization

For the steering application, the control objective is reference tracking, for which the actuation signal is always the required motor torque. Consequently, the reference signal for the motor is provided in either torque or current form, and the goal of the controller is to control the torque generated by the motor.

Since in (3) the torque-generating current ($i_q$) is not part of the measurement vector, the reference must be converted to a reference aligning with the motor control closed-loop. The rotor speed ($\omega$) affects the input $u_q$ that controls $i_q$, hence a mapping from the reference of $i_q$ ($i_{q_{ref}}$) to the $\omega$-domain is designed based on the coupling between the equations of the plant model. The resulting reference signal is a quasi-$\omega$ reference and henceforth will be coined $\xi$. Moreover, to better capitalize on the knowledge of load disturbance, its effect is taken into account in the reference mapping process by including both the $2^{nd}$ and $3^{rd}$ system equations.

To determine $\xi$ from $i_{q_{ref}}$, first a calculated rotor speed is expressed from the $2^{nd}$ equation of (1) using $i_{q_{ref}}$ and its derivative $\dot{i}_{q_{ref}}$, which gives

$$\bar{\omega} = \frac{L\dot{i}_{q_{ref}} + Ri_{q_{ref}} - u_q}{-\psi - Li_d}. \tag{9}$$

Then, substituting $\bar{\omega}$ into the $3^{rd}$ equation of (1) and taking the integral results in

$$\xi = \int \frac{3}{2}\frac{n_p\psi i_{q_{ref}}}{J} - \frac{\beta\bar{\omega} + T_l}{J}, \tag{10}$$

which is now a suitable input to the tracking controller.
The PMSM, after linearizing by feedback, can be controlled by any linear controller. For this purpose, the most common type is classic PI control, which is also applied in this paper. The control action is formulated as

$$v_d(t) = K_{p_d}e_d(t) + K_{i_d}\int_{t_0}^{t} e_d(t)\ dt, \tag{11}$$

$$v_q(t) = \tilde{K}_{p_q}\tilde{e}_q(t) + \tilde{K}_{i_q}\int_{t_0}^{t} \tilde{e}_q(t)\ dt, \tag{12}$$

where $K_{p_d}$ and $K_{i_d}$ are proportional and integral terms corresponding to $i_d$ and $\tilde{K}_{p_q}$ and $\tilde{K}_{i_q}$ are proportional and integral terms corresponding to $i_q$ and the error terms are $e_d = i_{d_{ref}} - i_d$ and $\tilde{e}_q = \xi - \omega$.

Substituting the feedback (8) and the virtual inputs (11) and (12) into the system model (1) gives the feedback-linearized closed-loop with PI control action:

$$\begin{aligned} \dot{i}_d &= \left(K_{p_d}e_d + K_{i_d}\int_{t_0}^{t} e_d\ dt\right), \\ \dot{i}_q &= \frac{\beta i_q}{J} - \frac{2\beta}{3\psi n_p J}(\beta\omega + T_l) \\ &\quad + \frac{2J}{3n_p\psi}\left(\tilde{K}_{p_q}\tilde{e}_q + \tilde{K}_{i_q}\int_{t_0}^{t} \tilde{e}_q\ dt\right), \\ \dot{\omega} &= \frac{3}{2}\frac{n_p\psi i_q}{J} - \frac{\beta\omega + T_l}{J}. \end{aligned} \tag{13}$$

The closed-loop control structure extended with the reference mapping described in (9) and (10) is presented in Fig. 1.

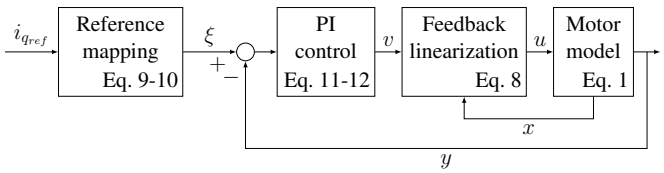


Fig. 1: Block diagram of the motor control structure.

**Remark 3.** *For the reference mapping task, the direct rearrangement of the $2^{nd}$ equation of the model* (1) *would be adequate. However, this solution poses numerical issues and does not account for abrupt changes in load dynamics.*

## V. Simulations

To demonstrate the benefits of the proposed approach, a standard PI-controlled motor model was used as a baseline structure. Moreover, the motor was embedded into a high-level mechatronic system, and the overall behaviour was also placed under scrutiny. For this purpose, a steering system with a rack position control objective was chosen. For the validation measurements, the high-level controller was of PID type. As we will see, the feasible tuning options of this controller and ultimately the entire system performance are influenced by the motor control behaviour. The overall control structure is presented in Fig. 2.

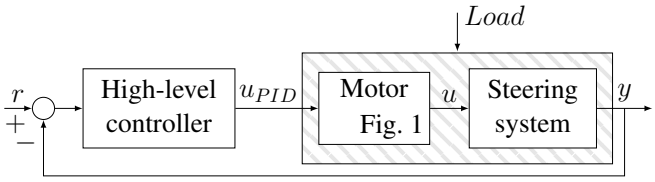


Fig. 2: Block diagram of the position control loop.

### A. Test procedures

The effectiveness of the controllers across various operating points is evaluated using step responses in four directions, as illustrated in Fig. 3. To cover all four motor quadrants on a motor torque - rotor speed map, this series of step inputs is evaluated corresponding to an increasing setpoint value ($s$). The time constant, representing the time it takes for the system to reach approximately 63.2% of its final value (dashed lines), serves as a key indicator of the system's responsiveness and stability.

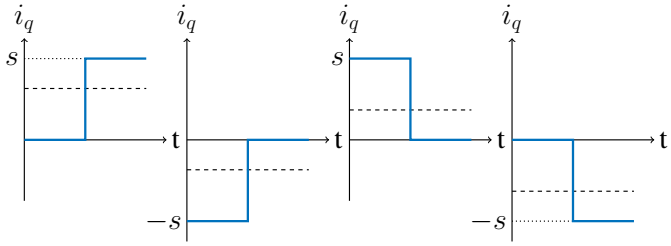


Fig. 3: Reference steps for motor control performance measurement.

The torque to current mapping was performed based on the linear relationship $T = i_q n_p \psi$, yielding a maximum of 250 A for the current.

To cover all possible combinations of $i_q$ and $\omega$ values, i.e. all operating points, an external load was applied and varied. This was necessary because the rotor speed is not controlled directly, rather it has a direct coupling with the torque-generating current. Given a constant load, the series of step inputs results in 'X'-shaped operating regimes. In Fig. 4, the series of step input operating points corresponding to different load points are highlighted.

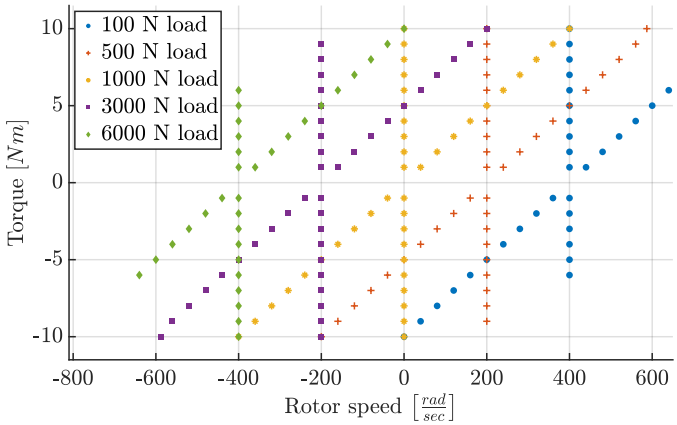


Fig. 4: Operating point series corresponding to a set of constant load values.

While the feedback-linearization-based method requires a load-dependent test procedure, the standard motor control with a PI controller can be validated by an external speed controller and a series of torque steps. Nevertheless, the two approaches are compared at the same operating points.

In Fig. 5, the reference torque steps and corresponding rotor speeds are presented, yielding two example operating points, each having its own time constant values, i.e. performance metrics.

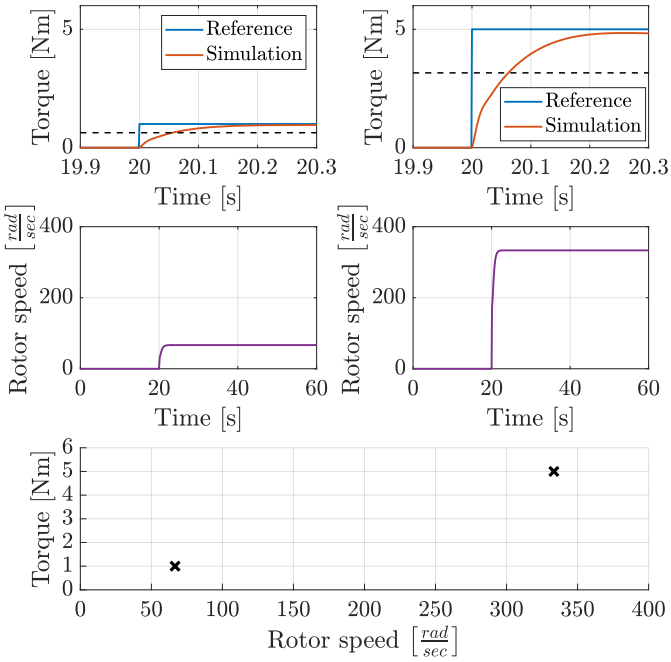


Fig. 5: Open-loop motor control performance measurements comparison of two controller settings (colours) corresponding to two operating points (columns).

The columns designate two specific operating points. The bottom subfigure is derived from the above operating points.

### B. Results

This subsection presents the validation results obtained from the prescribed test procedures and highlights the superiority of the proposed method in terms of motor dynamics, especially linearity. Fig. 6 illustrates the time constant of the motor for each operating point as the function of rotor speed and requested torque. An obvious advantage of the PI-controlled feedback linearized motor is its homogeneity over the entire operating range. In contrast, the standard PI-controlled model exhibits a high variation of motor responsiveness. Although in the nominal operating range, the performance was tuned similarly, in extreme conditions, the feedback-linearization method surpasses the basic solution.

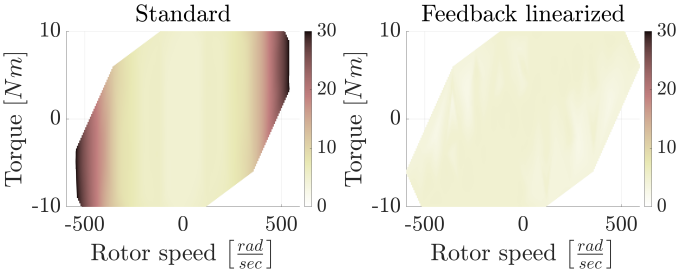


Fig. 6: Time constant of the motor in different operating regions.

Fig. 7 presents the step responses with linear PI control and feedback linearization for nominal (rotor speed: 65 $\frac{\text{rad}}{\text{sec}}$) and extremum (rotor speed: 500 $\frac{\text{rad}}{\text{sec}}$) operating conditions, respectively. Both solutions handle noisy measurement signals well. While under normal operation, the standard controller performs equally well, in more marginal scenarios (higher rotor speeds), feedback linearization outperforms the basic approach in terms of dynamics. It should be noted that the operating condition boundaries were designed so that no saturation effects would occur. In fact, the nominal 2 ms time constant behaviour is feasible in terms of control input in the entire operating region for the proposed method.

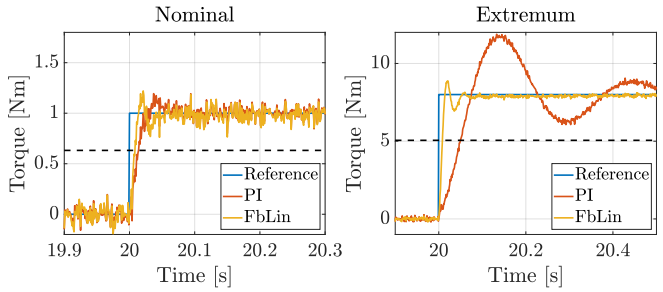


Fig. 7: Step response comparison in case of nominal and extremum operating conditions.

The PMSM motor behaviour was tested by aiding a generally linear steering system with a rack position control objective. Requirements towards such systems are usually very strict, leading to marginal controller settings potentially violating robust qualities. A common occurrence in such situations is the presence of oscillations, out of which a vastly undesirable one is the so-called 'shudder' effect caused by the poor dynamical behaviour of the motor. It is characterized by a 20 Hz relatively high amplitude vibration, given that high rotor speeds are maintained for a sufficiently long time.

Fig. 8 presents the pole-zero map of the closed-loop steering system. The colours denote different versions of the same system structure with increasing motor time constant. For a fixed linear controller, the slower the motor becomes, the closer the system moves to the positive half-plane, eventually crossing 0. The marginally stable pole-pair resides around 20 Hz, corresponding to the shudder effect.

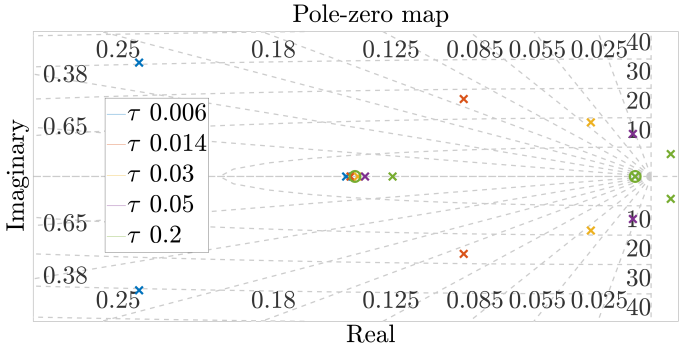


Fig. 8: Pole-zero map of the closed-loop high-level control system corresponding to increasing motor time constant.

Though these kinds of oscillations can be reduced by high-level controller tuning, strict requirements towards dynamic vehicle motion necessitate the use of the strongest setting possible, ultimately leaving the motor control loop in a degraded mode due to the small-gain theorem.

Moreover, the already nonlinear character of the motor is usually further enhanced by abrupt changes in dynamics moving along rotor speeds. The described method is supposed to overcome this problem by 'flattening' the rotor speed - motor current map.

With feedback linearization, the shudder effect can be significantly reduced even beside a strong position controller exhibiting high performance, as demonstrated in Fig. 9.

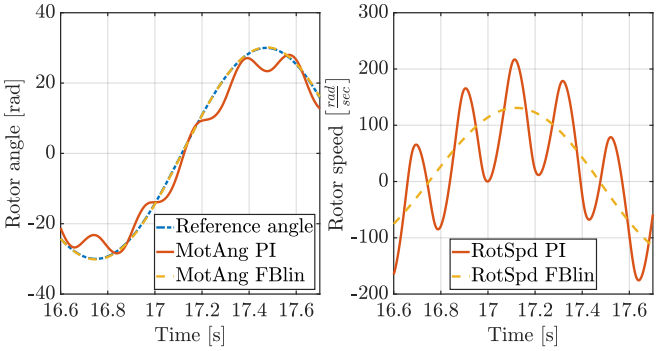


Fig. 9: Oscillatory behaviour comparison between standard PI motor control and feedback linearized control.

### C. Robustness analysis

For the sake of analysis, load estimation was modelled with the low-pass filter $H_{lpf}(s) = \frac{5}{\alpha s+5}$ where $\alpha$ is a parameter that can be adjusted to explore how changes in bandwidth frequency affect time differences at each operating point. Such an analysis may be useful to specify requirements against load estimation accuracy and bandwidth.

In Fig. 10, different simulation results are displayed, with dots representing the operating points. Green dots indicate operating points where the simulated signal accurately tracks the reference signal. In contrast, red dots represent cases where reference tracking fails due to various limitations.

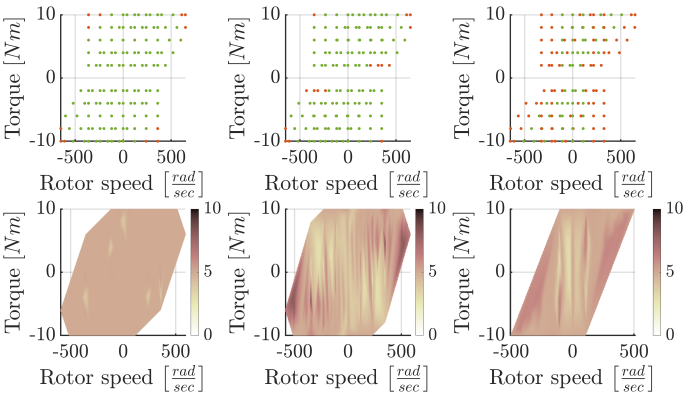


Fig. 10: Motor control performance and stability as a function of load estimation bandwidth. From left to right: 10 Hz - 1 Hz - 0.5 Hz.

On the leftmost subfigure, the estimator with the highest bandwidth was used, and as such, this test run returns the nominal torque-speed map with close to zero degraded operating points. However, as the bandwidth is limited, more and more invalid, that is, degraded or unstable operating points appear. In the corresponding bottom figures, the trend with increasing time constants (performance degradation) can be observed, and also, the invalid operating points are omitted, resulting in a much narrower stable operating range for the lower bandwidth estimators.

The bandwidth range of the load estimator was examined from 0.1 to 30 Hz according to Table II. The average time constants were included only for the cases in which no significant reduction in operating range had occurred.

TABLE II: Robustness analysis data for the load estimator.

| **Estimator bandwidth [Hz]** | **Unstable operating points** | **Average time constant [ms]** |
|---|---|---|
| 30 | 10 | 5.2 |
| 20 | 10 | 5.2 |
| 10 | 10 | 5.3 |
| 5 | 10 | 5.5 |
| 2 | 12 | 7.8 |
| 1 | 18 | NA |
| 0.5 | 75 | NA |
| 0.1 | 121 | NA |

## VI. Conclusion

The proposed approach, as indicated by validation measurements, has the potential to improve actuator control even when the objective is not well-suited to the model. In particular, when current/torque reference control is required as the only objective, the standard PMSM motor model does not admit a straightforward feedback linearization approach. For this reason, an indirect torque control method was proposed wherein a reference speed is calculated and the resulting feedforward speed controls the actual torque to its desired level. Linearization results in a significantly improved current control eliminating nonlinear character throughout the entirety of the operating region. This, in turn, allows for smoother and more stable operation. Moreover, this means that a higher-level control loop can withstand a higher level of disruptions, ultimately suggesting superior robustness qualities. With that said, a significantly larger effort must be taken to verify the robust performance and stability of the control loop in the presence of uncertain parameters and unmodelled dynamics. As a start, however, robustness against load estimation performance has been tested, and the initial results show fair behaviour. As another potential improvement, the validation tools could be extended to real-life systems.

## Acknowledgment

This research was supported by the Hungarian National Research, Development, and Innovation Office through the grant K-145934.

## References

[1] F. Amin, E. Sulaiman, and H. Soomro, "Field oriented control principles for synchronous motor," *International Journal of Mechanical Engineering and Robotics Research*, vol. 8, pp. 284–288, 01 2019.

[2] A. Hughes and B. Drury, *Variable Frequency Operation of Induction Motors*, 12 2013, pp. 205–253.

[3] L. Sepulchre, M. Fadel, M. Pietrzak-David, and G. Porte, "Flux-weakening strategy for high speed pmsm for vehicle application," in *2016 International Conference on Electrical Systems for Aircraft, Railway, Ship Propulsion and Road Vehicles & International Transportation Electrification Conference (ESARS-ITEC)*, 2016, pp. 1–7.

[4] Z. Wu, Y. Shen, T. Pan, and Z. Ji, "Feedback linearization control of pmsm based on differential geometry theory," in *2010 5th IEEE Conference on Industrial Electronics and Applications*, 2010, pp. 2047–2051.

[5] C. Lascu, I. Boldea, and F. Blaabjerg, "Direct torque control via feedback linearization for permanent magnet synchronous motor drives," in *2012 13th International Conference on Optimization of Electrical and Electronic Equipment (OPTIM)*, 2012, pp. 338–343.

[6] H. Sira-Ramirez, J. Linares Flores, C. Garcia-Rodriguez, and M. Contreras, "On the control of the permanent magnet synchronous motor: An active disturbance rejection control approach," *IEEE Transactions on Control Systems Technology*, vol. 22, pp. 2056–2063, 06 2014.

[7] H. K. Khalil, *Nonlinear systems; 3rd ed.* Upper Saddle River, NJ: Prentice-Hall, 2002.

[8] Z. Téczely, C. Fazekas, and B. Kiss, "Lpv control of systems via nonlinear actuator dynamics mapping," in *2024 28th International Conference on Methods and Models in Automation and Robotics (MMAR)*, 2024, pp. 205–210.

[9] W. Leonhard, *Control of electrical drives*. Springer Science & Business Media, 2001.

[10] A. Isidori, M. Thoma, E. D. Sontag, B. W. Dickinson, A. Fettweis, J. L. Massey, and J. W. Modestino, *Nonlinear Control Systems*, 3rd ed. Berlin, Heidelberg: Springer-Verlag, 1995.